

Mitochondrial defects and heterogeneous cytochrome *c* release after cardiac cold ischemia and reperfusion

Andrey V. Kuznetsov,¹ Stefan Schneeberger,¹ Rüdiger Seiler,¹ Gerald Brandacher,¹ Walter Mark,¹ Wolfgang Steurer,¹ Valdur Saks,² Yves Usson,³ Raimund Margreiter,¹ and Erich Gnaiger¹

¹Department of Transplant Surgery, D. Swarovski Research Laboratory, University Hospital Innsbruck, A-6020 Innsbruck, Austria; ²Laboratory of Bioenergetics, Joseph Fourier University, Grenoble Cedex 9; and ³Techniques de l'Imagerie de la Modelisation et de la Cognition Laboratory, UMR5525 Centre National de la Recherche Scientifique, Institute Albert Bonniot, Grenoble 38706, France

Submitted 21 July 2003; accepted in final form 19 December 2003

Kuznetsov, Andrey V., Stefan Schneeberger, Rüdiger Seiler, Gerald Brandacher, Walter Mark, Wolfgang Steurer, Valdur Saks, Yves Usson, Raimund Margreiter, and Erich Gnaiger. Mitochondrial defects and heterogeneous cytochrome *c* release after cardiac cold ischemia and reperfusion. *Am J Physiol Heart Circ Physiol* 286: H1633–H1641, 2004; 10.1152/ajpheart.00701.2003.—Mitochondria play a critical role in myocardial cold ischemia-reperfusion (CIR) and induction of apoptosis. The nature and extent of mitochondrial defects and cytochrome *c* (Cyt *c*) release were determined by high-resolution respirometry in permeabilized myocardial fibers. CIR in a rat heart transplant model resulted in variable contractile performance, correlating with the decline of ADP-stimulated respiration. Respiration with succinate or *N,N,N',N'*-tetramethyl-*p*-phenylenediamine dihydrochloride (substrates for complexes II and IV) was partially restored by added Cyt *c*, indicating Cyt *c* release. In contrast, NADH-linked respiration (glutamate+malate) was not stimulated by Cyt *c*, owing to a specific defect of complex I. CIR but not cold ischemia alone resulted in the loss of NADH-linked respiratory capacity, uncoupling of oxidative phosphorylation and Cyt *c* release. Mitochondria depleted of Cyt *c* by controlled hypoosmotic shock provided a kinetic model of homogenous Cyt *c* depletion. Comparison to Cyt *c* control of respiration in CIR-injured myocardial fibers indicated heterogeneity of Cyt *c* release. The complex I defect and uncoupling correlated with heterogeneous Cyt *c* release, the extent of which increased with loss of cardiac performance. These results demonstrate a complex pattern of multiple mitochondrial damage as determinants of CIR injury of the heart.

respiration; heart preservation; complex I injury; permeabilized myocardial fibers

PROLONGED ISCHEMIA and subsequent reperfusion of the heart result in energy deprivation, significant damage of mitochondria, and lead to cardiac cell death and irreversible heart injury. Mitochondrial function is critical in heart injury after ischemia-reperfusion and ischemic and pharmacological preconditioning (9, 10, 49). Increased production of reactive oxygen species (ROS) by mitochondria on reperfusion leads to oxidative stress, including mitochondrial permeability transition, loss of mitochondrial membrane potential, and cytochrome *c* release (35). Moreover, ROS interact with physiological signal transducers (44). In the context of organ preservation and transplantation, ischemia-reperfusion injury can be significantly delayed by hypothermic organ storage. While the alterations of mitochondrial function and cytochrome *c* depletion

after myocardial normothermic ischemia are well documented (32, 33), less is known concerning the mechanisms of mitochondrial damage after cold ischemia (CI)-reperfusion (CIR). Prolonged CI and rewarming-reperfusion jeopardize myocardial capacity to regenerate energy by mitochondrial oxidative phosphorylation (22, 47). Extended cardiac cold storage correlates with progressive loss of mitochondrial function before (43) and after reperfusion (22, 28, 50). The exact relationship between mitochondrial injury and loss of cardiac performance after CIR, however, remains to be elucidated. In our study, normothermic blood reperfusion was used as a model for clinical heart transplantation.

Cytochrome *c* release from mitochondria after ischemia-reperfusion (3) and activation of the caspase pathway with the consequent induction of apoptosis have been studied intensively (15, 48). The metabolic consequences, however, of cytochrome *c* release from mitochondria are poorly understood. This is a potentially important issue because apoptosis requires ATP, which is mainly produced in mitochondrial oxidative phosphorylation. Availability of ATP during reoxygenation is a prerequisite for apoptosis; hence, energy deprivation shifts the cell toward necrosis (31).

Imaging techniques have revealed the coexistence of mitochondria with different redox or membrane potentials (6, 29). Heterogeneous mitochondrial damage is characteristic for various pathologies (27, 42). Recently, direct proof was obtained for heterogeneous cytochrome *c* release and cellular mosaicism of respiratory changes (16). To our knowledge, the problems of heterogeneous mitochondrial damage and heterogeneity of cytochrome *c* release have not yet been addressed after CIR of the heart. Cytochrome *c* release potentially induces apoptosis or necrosis by activation of caspase pathways or by diminished cellular ATP levels due to inhibition of oxidative phosphorylation. Thus heterogeneity and the extent of cytochrome *c* release are critical for regulating the switch between development of apoptosis or necrosis.

Our study on mitochondrial CIR injury shows that stimulation of respiration by added cytochrome *c* strongly depends on the mitochondrial substrate. Analysis of cytochrome *c* kinetics with succinate and *N,N,N',N'*-tetramethyl-*p*-phenylenediamine dihydrochloride (TMPD)+ascorbate demonstrated heterogeneity of mitochondrial cytochrome *c* depletion after CIR. Taken together, these results show that CIR of the heart

Address for reprint requests and other correspondence: E. Gnaiger, Dept. of Transplant Surgery, D. Swarovski Research Laboratory, Univ. Hospital Innsbruck, Innrain 66/6, A-6020 Innsbruck, Austria (E-mail: erich.gnaiger@uibk.ac.at).

The costs of publication of this article were defrayed in part by the payment of page charges. The article must therefore be hereby marked "advertisement" in accordance with 18 U.S.C. Section 1734 solely to indicate this fact.

induces specific damage of respiratory complex I, uncoupling of mitochondria, and heterogeneous cytochrome *c* release, showing the multifactorial nature of mitochondrial injury. These aspects of mitochondrial injury correlated with the loss of cardiac contractile function after reperfusion but were absent after CI alone.

MATERIALS AND METHODS

Animals. Male Lewis rats (200–250 g) were used in a syngeneic heart transplantation model. Animals were housed under standard conditions with free access to diet and water according to the Austrian Animal Care Law. All experiments were performed with approval of the National Animal Welfare Committee and followed the National Institutes of Health *Guide for the Care and Use of Laboratory Animals* (NIH Publication 85-23, Revised 1985).

Cardiac preservation and transplantation. All procedures were performed while the animals were under anesthesia with pentobarbital given intraperitoneally at a dose of 0.5 mg/kg. Heterotopic cardiac transplantation was performed according to Ono and Lindsey (38). After intravenous injection of heparin into the donor (1 IU/g), hearts were flushed in a retrograde fashion via the ascending aorta with 10 ml of ice-cold preservation solution and stored on ice for 10 h in the same preservation solution. Before transplantation, grafts were again flushed with 10 ml of ice-cold preservation solution through an intraaortic cannula. During revascularization, grafts were wrapped in moist gauze and intermittently cooled with cold preservation solution. The donor aorta and pulmonary artery were anastomosed to the recipient abdominal aorta and inferior vena cava. Vascular clamps were removed and hearts were reperfused after 60 min of anastomosis. After reperfusion for 24 h, relaparotomy was carried out while the animals were under terminal anesthesia. Graft function was evaluated by direct palpation of the graft as well as macroscopic and binocular inspection as follows: *score 1*, fibrillations visible by binocular assessment but not detectable by palpation; *score 2*, weak or partial contractions detectable by palpation; *score 3*, homogenous contractions of both ventricles at reduced frequency and intensity; *score 4*, normal contraction intensity and frequency. Heart scores were stable at *score 4* in control transplants without ischemia, whereas after CIR scores ranged from 4 to 1, i.e., from normal to zero graft function.

A cold ischemic period of 10 h was chosen on the basis of previous studies, which showed that this represents a critical preservation time, leading to variable posts ischemic heart function between the limits of normal and zero performance. The reperfusion time of 24 h was considered for the stable assessment of graft function. The graft function scores were estimated by two experimentators (surgeons) in blinded manner, i.e., the scoring was completed before a different experimenter started the respirometric experiments.

Portions of each heart were frozen in liquid nitrogen and stored at -80°C until homogenate preparation. Either University of Wisconsin (UW) solution (ViaSpan) or histidine-tryptophan-ketoglutarate (HTK) solution (Custodiol) was used for cold flush and preservation of grafts. Application of two established preservation solutions was designed to increase the range of ischemia-reperfusion injury, but alterations of mitochondrial respirometric and enzymatic function and cardiac score (heart contractile performance) were indistinguishable in terms of average and variability of results obtained with the two solutions. Cardiac scores were 2.6 ± 1.3 ($n = 7$) for UW and identical for HTK (2.6 ± 0.9 ; $n = 8$; $P > 0.05$), with similar distribution for the two preservation solutions (2, 1, 2, and 2 hearts yielding *scores 1–4* with HTK; 1, 2, 4, and 1 hearts yielding *scores 1–4* with UW).

Experimental groups. In the CI group ($n = 3$), hearts were flushed, cold stored for 10 h, flushed again, and subjected to second ischemia for 60 min with topic cooling of the graft. In the CIR group ($n = 15$), this CI protocol was followed by transplantation and 24 h of reperfusion. Hearts serving as baseline controls ($n = 7$) were extracted, flushed with ice-cold UW solution, and used for sample preparation.

Preparation of permeabilized myocardial fibers. To avoid artifacts of selection of intact organelles and of mitochondrial preparation, and to minimize the amount of tissue, we applied the technique of permeabilized muscle fibers without isolation of mitochondria by mechanical dissection of muscle tissue in relaxing solution on ice (29). From a 50-mg tissue sample, fiber bundles were prepared and nearly all fibers were used for usually five replicate experiments, without selection for more or less damaged tissue. The relaxing solution contained (in mM) 2.77 CaK₂EGTA, 7.23 K₂EGTA (free Ca²⁺ concentration 0.1 μM), 20 imidazole, 20 taurine, 6.56 MgCl₂, 5.77 ATP, 15 phosphocreatine, 0.5 dithiothreitol, and 50 K-MES, pH 7.1. Myocardial fibers were permeabilized by gentle agitation for 30 min at 4°C in the relaxing solution supplemented with 50 $\mu\text{g}/\text{ml}$ saponin. Fibers were washed in ice-cold respiration medium (see below) by agitation for 10 min and were kept in this medium (see below) until respirometric assay.

Depletion of mitochondrial cytochrome *c* was achieved by selective disruption of the mitochondrial outer membrane by the previously validated technique of controlled hypoosmotic shock (41). Permeabilized fibers from control hearts (no ischemia, no reperfusion) were incubated for 30 min at 0°C in hypoosmotic medium (30 mosmol/l), prepared by dilution of relaxing solution. The fibers were then transferred into high ionic strength solution (0.15 M KCl, 20 mM KH₂PO₄, and 20 mM HEPES, pH 7.4) and incubated for 30 min at 4°C. After such treatment, transport and catalytic functions of the inner mitochondrial membrane and respiratory complexes remain preserved. After the addition of saturating concentrations of external cytochrome *c* respiration remains coupled, as shown by normal ADP control, and mitochondrial NADH retention was indicated by fluorescence microscopy (data not shown).

High-resolution respirometry. Respiration was measured at 30°C in titration-injection respirometers (Oroboros, Oxygraph; Innsbruck, Austria) (12). The respiration medium consisted of 110 mM sucrose, 60 mM K-lactobionate, 0.5 mM EGTA, 1 g/l BSA essentially fatty acid free, 3 mM MgCl₂, 20 mM taurine, 10 mM KH₂PO₄, 20 mM K-HEPES, pH 7.1 (14). The O₂ solubility of this medium was taken as 10.5 $\mu\text{M}/\text{kPa}$. The software DatLab (Oroboros) was used for data acquisition and analysis. Respiratory rates (oxygen fluxes) were expressed per milligram of dry weight. Steady-state cytochrome *c* kinetics was measured in cytochrome *c* depleted permeabilized myocardial fibers, using mitochondrial medium with 1 mM ADP and 10 mM succinate/0.5 μM rotenone or 0.5 mM TMPD + 2 mM ascorbate/5 μM antimycin A (13). Chemical background controls due to autoxidation of TMPD and ascorbate were determined in the presence of different concentrations of cytochrome *c* (0–87 μM) over the entire experimental oxygen range. Cytochrome *c* stimulated respiration was fully inhibited by 1 mM KCN, to the level of oxygen flux corresponding to the instrumental and chemical background (40). This validates the background corrections that were routinely applied as a function of the concentrations of TMPD, ascorbate, cytochrome *c*, and dissolved oxygen (13).

Confocal microscopy of mitochondrial flavoproteins. Isolated saponin permeabilized fiber bundles were fixed at both ends in a Flexiperm chamber (Heraeus; Hanau, Germany). Respiration medium (200 μl) was then added. Fully oxidized state of mitochondrial flavoproteins was achieved by substrate deprivation and equilibration of the medium with air at room temperature. Digital images of mitochondrial flavoproteins were acquired with a confocal microscope (model LSM510-NLO, Zeiss) with a $\times 40$ objective water-immersion lens (numerical aperture 1.2). The autofluorescence was excited with the 488-nm line of an Argon laser and collected through a 510-nm dichroic beam splitter and a 505–550 nm band-pass filter. Cross-sections were obtained using the XZ scanning facility of the confocal microscope. The Z step was 0.15 μm on average.

Enzyme activities. Frozen tissue samples were placed into ice-cold 0.1 M phosphate buffer, pH 7.4, and homogenized for 30 s with an Ultra-Turrax homogenizer at maximum speed. The activities of mi-

tochondrial NADH:ubiquinone oxidoreductase (complex I) and citrate synthase were assayed spectrophotometrically at 30°C (19, 46). For the complex I assay, homogenates (30 mg/ml) were centrifuged at 70,000 g for 30 min (4°C). The resultant pellet was then suspended in the same volume of phosphate buffer and sonicated for 40 s on ice.

Chemicals. Cytochrome *c* (horse heart) was obtained from Boehringer Mannheim (Germany). Taurine and inorganic salts were from Merck (Germany). Lactobionic acid was obtained from Fluka Chemie (Germany). All other chemicals were from Sigma (Germany). BSA was essentially fatty acid free.

Data analysis. All data are presented as means \pm SD. Statistical analyses were performed using Student's *t*-test, and $P < 0.05$ was taken as the level of significance.

RESULTS

Multiple mitochondrial defects after CIR. Mitochondrial respiration in the presence of substrates (state 2) is stimulated by the addition of ADP (state 3) by a factor known as the respiratory control ratio ($RCR_{3/2}$). With glutamate and malate as substrates for mitochondrial complex I, this ADP control ratio was 8.2 ± 1.5 ($n = 7$) in permeabilized fibers of baseline control hearts. The ADP control ratio was not significantly reduced after CI without reperfusion (CI; 6.9 ± 0.8 , $n = 3$). After CIR, however, the ADP respiratory control ratio declined progressively with the loss of cardiac performance (Fig. 1A). Although the decrease of the $RCR_{3/2}$ is consistent with uncoupling of oxidative phosphorylation, a low ratio does not afford a sufficient proof for mitochondrial uncoupling. In fact, uncoupling alone would cause an increase of respiration in the absence of ADP (state 2). On the contrary, state 2 respiration declined significantly with cardiac score after CIR (data not shown). This observation and low ADP control ratios were explained by the specific loss of enzyme activity of respiratory complex I (NADH:ubiquinone oxidoreductase) observed after CIR (Fig. 1B). Respiratory capacity of permeabilized fibers with glutamate+malate declined as a nonlinear function of complex I activity in myocardial homogenates (Fig. 1C). Under these conditions, the low $RCR_{3/2}$ is no indicator for uncoupling.

The activity of citrate synthase, a marker enzyme for the mitochondrial matrix, was independent of cardiac score (Fig. 1B). Citrate synthase activity of all CIR hearts averaged 85% of enzyme activity in baseline controls. The relatively good preservation of citrate synthase activity indicates that total mitochondrial content remained largely unchanged, and citrate synthase activity was relatively resistant against CIR injury. In contrast, complex I activity was reduced to 53% of baseline controls in CIR hearts of scores 3 and 4, and declined to 26% of controls in grafts of scores 1 and 2 (Fig. 1B).

Cytochrome *c* release from mitochondria inhibits respiration due to limitation of electron transport to cytochrome *c* oxygenase. Depending on the localization of enzymatic defects, the extent of inhibition may change when measured through different segments of the respiratory chain. Consequently, the stimulatory effect of cytochrome *c* addition was tested separately for complex I, II, and IV respiration (shaded sections in Fig. 2, A–C). After CI without reperfusion, respiratory capacity remained unchanged with glutamate + malate (Fig. 2D) but declined significantly with succinate and TMPD+ascorbate either in the presence or in the absence of cytochrome *c* (Fig. 2, E and F). After CIR, however, complex I respiratory capacity declined as a function of heart score both with and

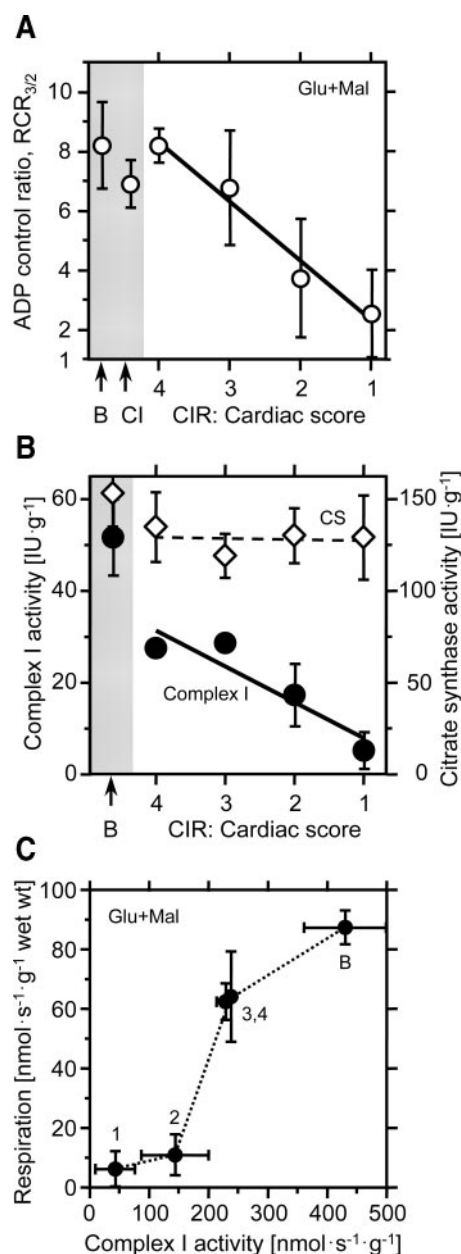


Fig. 1. Respiratory defects and complex I damage after cold ischemia (CI)-reperfusion (CIR). A: ADP control ratio of respiration to state 2 and state 3 ($RCR_{3/2}$) with 10 mM glutamate and 5 mM malate (NADH-linked respiration) in baseline (B) control hearts, after CI and CIR. Values are means \pm SD (B, $n = 7$; CI, $n = 3$; CIR, $n = 3$ to 4 in each score). B: activity of complex I (NADH:ubiquinone-1 oxidoreductase; ●) and citrate synthase (CS; ◇). C: dependence of ADP-stimulated respiration and complex I activity. To obtain equivalent units for both axes, respiration was expressed per gram of wet weight (using a wet weight-to-dry weight ratio of 5; Ref. 50), and enzyme activity was expressed in O_2 equivalents per gram of wet weight.

without added cytochrome *c* (Fig. 2D). The absence of a stimulatory effect of exogenous cytochrome *c* at various degrees of complex I injury indicates full control by complex I, which overrides any effect of cytochrome *c* depletion under these conditions of multiple mitochondrial damage. Without added cytochrome *c*, a similar decline of respiration with graft function was seen with succinate or TMPD (Fig. 2, E and F; open symbols). In the presence of cytochrome *c*, however, no

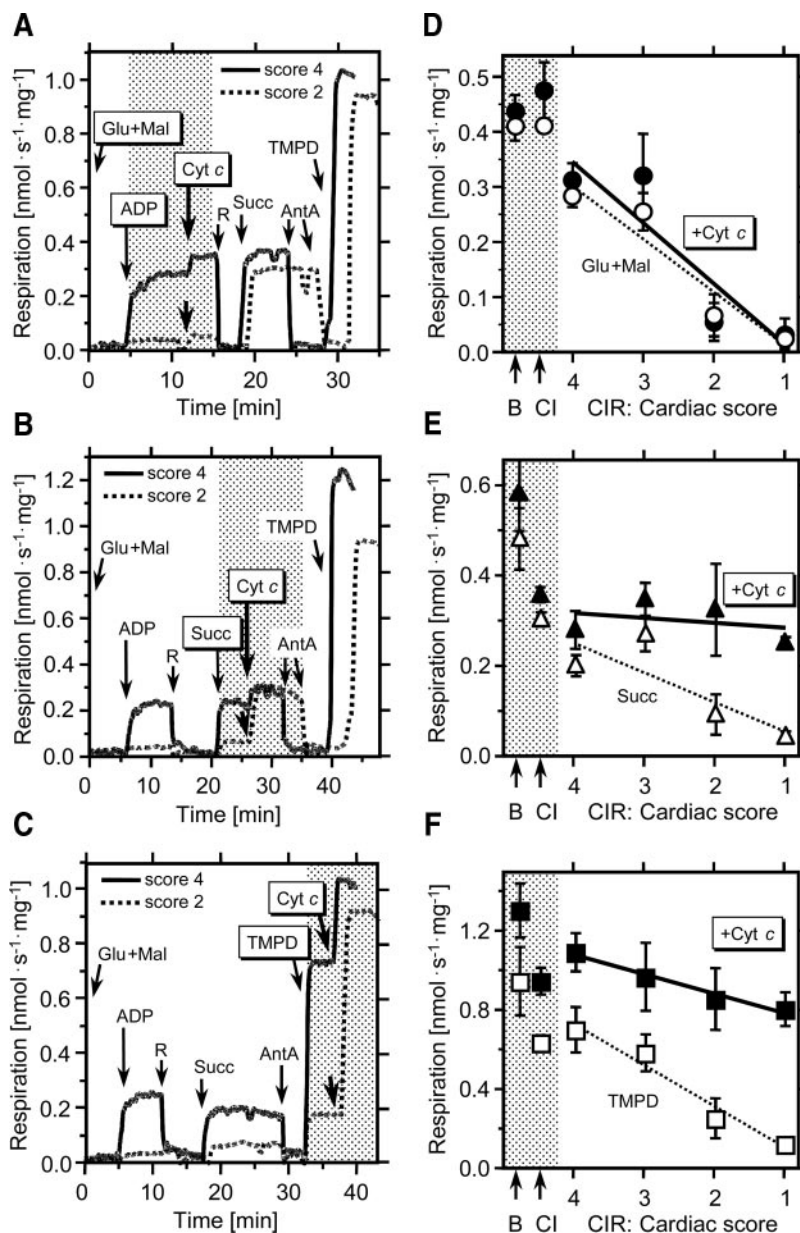


Fig. 2. Mitochondrial respiration through different segments of the electron transport chain after cold ischemia-reperfusion, with particular emphasis on stimulation by cytochrome *c*. *A–C*: representative traces of oxygen flux using a multiple substrate-inhibitor titration protocol with stimulation by 1 mM ADP, cytochrome *c*, and various substrates. Cytochrome *c* (Cyt *c*, 10 μ M; shaded sections) was added at the stage of complex I respiration (*A*; Glu+Mal; 10 mM glutamate and 5 mM malate), complex II respiration [*B*; Succ; 10 mM succinate after inhibition of complex I with 0.5 μ M rotenone (R)], and complex IV respiration [*C*; 0.5 mM *N,N,N',N'*-tetramethyl-*p*-phenylenediamine dihydrochloride (TMPD) and 2 mM ascorbate after inhibition of complex III with 5 μ M antimycin A (AntA)]. Experiments are shown for hearts with *score 4* (full trace) and *score 2* (dotted trace). *D–F*: complexes I, II, and IV respiration after addition of ADP (state 3; open symbols) and further stimulation by cytochrome *c* (state 3c; solid symbols) in baseline (*B*) control hearts, after CI, and as a function of cardiac score after CIR.

further decline of respiratory capacity of complexes II and IV was observed with the loss of cardiac performance, and the stimulatory effect of cytochrome *c* increased with the decline in cardiac score (Fig. 2, *E* and *F*; closed symbols). The addition of cytochrome *c* restored respiration to the level of the CI group. In contrast, cytochrome *c* stimulation of complex I respiration was very small under all conditions (Fig. 2*D*). This reflects the fact that respiration with glutamate+malate was severely limited by the enzymatic defect of complex I (Fig. 1*B*), which reduced respiratory control by both cytochrome *c* and ADP.

On the basis of these results, a respiratory protocol was designed for discrimination between inhibitory effects of CIR-induced enzymatic injuries (including cytochrome *c* depletion) and uncoupling on the low RCR. This requires a respiratory reference state to be established in which electron transport is not impaired. Whereas complex IV respi-

ration might be favored in this respect, owing to its relatively high stability after CIR, this advantage is offset by the low phosphorylation stoichiometry of cytochrome *c* oxidase, which yields low adenylate control ratios relative to complex I or II respiration. This and the specific defect of complex I, therefore, suggested complex II respiration as a basis for the uncoupling test. Importantly, cytochrome *c* was added before stimulation by ADP to avoid the compounding effect of cytochrome *c* depletion (Fig. 3*A*). Under these conditions, uncoupling was indicated by 1) the pronounced increase of respiration in the absence of adenylates (state 2c), and 2) the significant decrease of the scope for ADP stimulation with progressive loss of heart function. This resulted in a decline of the RCR_{3c/2c} to the minimal value of 1.0 at a cardiac score of 1 (Fig. 3*B*). These indicators of uncoupling increased with an increasing extent of stimulation of respiration by cytochrome *c*.

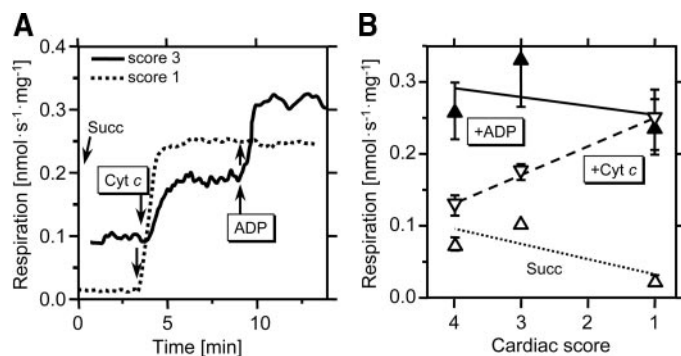


Fig. 3. Uncoupling of mitochondria and cytochrome *c* depletion correlate with cardiac score after CIR. A: representative traces of respiration with succinate for hearts with *score* 3 (full trace) and *score* 1 (dotted trace). B: respiration in state 2 (dotted line), state 2c (+10 μ M cytochrome *c*; dashed line) and state 3c (+1 mM ADP; full line) after CIR as a function of cardiac score. State 2c rate increased with loss of cardiac function, and the scope for ADP stimulation declined to zero.

Cytochrome *c* kinetics of mitochondrial respiration and heterogeneous cytochrome *c* release after cardiac CIR. The extent of inhibition of mitochondrial respiration by cytochrome *c* depletion was analyzed in the context of steady-state kinetics with increasing concentrations of cytochrome *c* performed with cytochrome *c* depleted myocardial fibers. To study cytochrome *c* kinetics, it was necessary to remove endogenous cytochrome *c* by controlled hypoosmotic shock and thus provide access for externally added cytochrome *c* to cytochrome *c* oxidase. In the absence of external cytochrome *c*, oxygen flux (state 3) is inhibited relative to cytochrome *c*-stimulated respiration (state 3c), depending on the extent of cytochrome *c* depletion. The ratio of state 3 and state 3c respiration (cytochrome *c* control ratio, $R_{CR_{3/3c}}$), therefore, reflects the loss of respiratory capacity due to cytochrome *c* release. The addition of 10 μ M cytochrome *c* resulted in a 5- to 7-fold stimulation of respiration in the presence of ADP and succinate. The correspondingly low $R_{CR_{3/3c}}$ ratio of 0.19 reflects the respiratory depression by cytochrome *c* depletion, comparable to the most severe CIR injury at a cardiac score of 1. This large extent of cytochrome *c* stimulation is directly related to cytochrome *c* release, as shown after warm ischemia (3, 4), treatment with proapoptotic protein Bax (1) and hypoosmotic shock (41). In addition, the selectivity of the controlled hypoosmotic treatment was validated by confocal imaging. Figure 4, A–D, shows the autofluorescence of mitochondrial flavoproteins in controls (Fig. 4, A and C) and cytochrome *c*-depleted myocardial fibers (Fig. 4, B and D). The regular mitochondrial arrangement was not changed after hypoosmotic shock and cytochrome *c* extraction, despite the remarkable swelling of the matrix space and rupture of the outer mitochondrial membrane (41). Moreover, the two photon confocal imaging technique revealed a clear colocalization of mitochondrial flavoprotein and NADH fluorescence across myocardial fibers (not shown).

Cytochrome *c* kinetics with succinate was compared with cytochrome *c* kinetics with TMPD+ascorbate, aiming to include both conditions where cytochrome *c* exerted significant respiratory control after CIR (Fig. 2, E and F). In this comparison, we distinguish respiration with succinate as flux (*J*) through the multistep pathway, and respiration with TMPD+ascorbate as reaction velocity (*v*) through the isolated

step of complex IV. Analogous to the apparent Michaelis-Menten constant (K_m') for cytochrome *c* in the single enzyme step, c_{50} is defined as the cytochrome *c* concentration at which flux through the pathway of succinate respiration is stimulated by 50% (13). Figure 4, E and F, shows the dependence of *J* and *v* in permeabilized and cytochrome *c*-depleted fibers as a function of cytochrome *c* concentration. Cytochrome *c* kinetics was entirely different with succinate compared with TMPD+ascorbate. Oxygen flux with succinate was monophasic hyperbolic, taking into account the linear inhibition of respiration observed at cytochrome *c* concentrations >10 μ M (Fig. 4F; Ref. 13). With TMPD+ascorbate, cytochrome *c* kinetics in permeabilized muscle fibers was biphasic (Table 1), and was fitted to a double rectangular equation fully comparable to isolated mitochondria (13).

Figure 5A summarizes the effect of externally added cytochrome *c* (10 μ M) in terms of cytochrome *c* control ratios, $R_{CR_{3/3c}}$, in permeabilized fibers after CIR, which were not treated by hypoosmotic shock. When measured with succinate or TMPD+ascorbate, $R_{CR_{3/3c}}$ did not change after CI but declined after CIR as a function of cardiac score, clearly demonstrating progressive cytochrome *c* release. Cytochrome *c* kinetics described above was used for simulating various degrees of cytochrome *c* depletion, expressed as respiratory cytochrome *c* control ratios, $R_{CR_{3/3c}}$, in a homogenous and heterogeneous system (Fig. 5B). For the model of homogenous cytochrome *c* release, $R_{CR_{3/3c}}$ ratios were obtained as a continuous function of initial cytochrome *c* concentration, x [μ M], for succinate, $R_{CR_{3/3c}}(\text{Succ}) = j_x/j_{x+10}$, and for TMPD, $R_{CR_{3/3c}}(\text{TMPD}) = v_x/v_{x+10}$. At any given cytochrome *c* concentration, the corresponding oxygen fluxes, j_x and v_x , as well as j_{x+10} and v_{x+10} , were calculated from the kinetic parameters for permeabilized myocardial fibers (Table 1). Owing to the different cytochrome *c* kinetics with succinate and TMPD, $R_{CR_{3/3c}}(\text{Succ})$ was a nonlinear function of $R_{CR_{3/3c}}(\text{TMPD})$ in the homogeneous model (Fig. 5B; solid line). In contrast, fully heterogeneous cytochrome *c* release, i.e., a simple mixture of intact and completely cytochrome *c* depleted mitochondria (hypothetical system where no partially cytochrome *c* depleted mitochondria exist), yields a strictly linear relation between the $R_{CR_{3/3c}}$ ratios for succinate and TMPD+ascorbate. This theoretical relationship for fully heterogeneous cytochrome *c* release is shown by the dashed line in Fig. 5B. By comparison, the data obtained with myocardial fibers from hearts subjected to CIR or CI (Fig. 5B; solid circles) show a relation between $R_{CR_{3/3c}}(\text{Succ})$ and $R_{CR_{3/3c}}(\text{TMPD})$, which is close to the theoretical linear relationship and does not overlap with the nonlinear relation for the homogeneous system (the SD for the means shown by closed circles in Fig. 5 averaged 0.06, and varied by ± 0.03). These results suggest that cytochrome *c* release was not homogeneously distributed over the mitochondrial population after CIR.

DISCUSSION

Previous studies (22, 28) of the isolated perfused heart point to the link between decreased mitochondrial and cardiac function after cold preservation and reperfusion. We found distinct patterns of mitochondrial injuries, involving multiple damage and different patterns of injury after CIR compared with cold ischemia alone. Capacities of complex II and IV respiration,

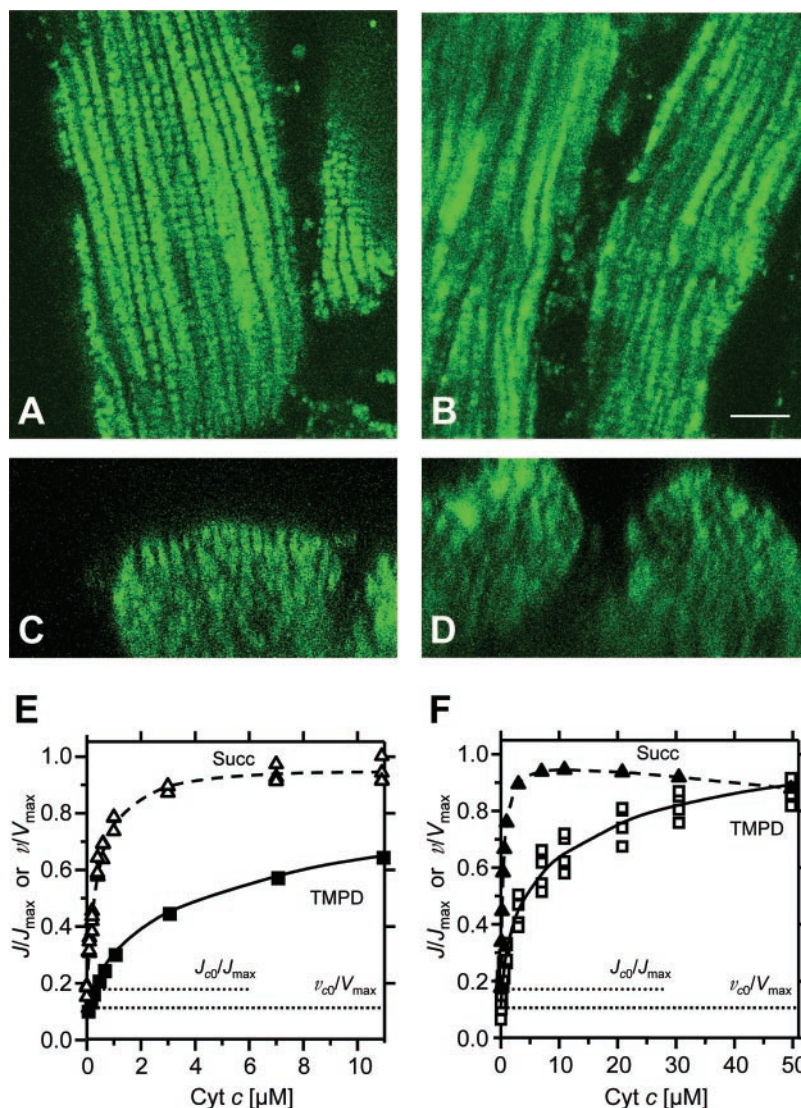


Fig. 4. Cytochrome *c* depletion by controlled hypoosmotic treatment of myocardial fibers. *A* and *B*: Confocal images of mitochondrial flavoproteins within controls (*A*) and after cytochrome *c* depletion (*B*). *C* and *D*: corresponding cross sections (XZ scanning). Bar, 10 μm . *E* and *F*: cytochrome *c* kinetics of respiration in cytochrome *c* depleted fibers, with succinate or TMPD+ascorbate as substrates. Total maximum fluxes (J_{max}) and reaction velocities (V_{max}) were used for normalization of flux (J) through the respiratory chain from complex II to IV (Succ; triangles, dashed lines) or reaction velocity (v) through the isolated step of complex IV (TMPD; squares, full lines). Open symbols show separate experiments, closed symbols are corresponding averages ($n = 4$). Data are shown in two ranges of cytochrome *c* concentrations, up to 11 μM (*E*) and 51 μM (*F*). J_{c_0} , flux at zero-added cytochrome *c* concentration.

measured after addition of cytochrome *c*, declined to 62% and 73% of baseline controls after CI. Effects of reperfusion on respiratory capacities (51% and 71% of baseline controls for succinate and TMPD, respectively) were not significant nor was there any correlation with contractile heart function. Sim-

ilarly, no changes in the activity of citrate synthase were detected with respect to cardiac function upon CIR, although activity was depressed on average to 85% of baseline controls (Fig. 1B). This is comparable to the decrease of citrate synthase activity to 79% of controls after 12 h of cold storage of the

Table 1. Parameters of cytochrome *c* kinetics with substrates for complex I and IV in cytochrome *c*-depleted permeabilized fibers and isolated mitochondria of heart

Preparation	TMPD + Ascorbate							
	Succinate			High affinity		Low affinity		
	c_{50} , $\mu\text{mol/l}$	ΔJ_{max}	J_{c_0}	$K'_{m,h}$, $\mu\text{mol/l}$	$\Delta V_{\text{max,h}}$	$K'_{m,l}$, $\mu\text{mol/l}$	$\Delta V_{\text{max,l}}$	v_{c_0}
Permeabilized fibers	0.41 ± 0.04	0.63 ± 0.14	0.13 ± 0.01	$0.88 \pm 0.23^*$	0.58 ± 0.16	12.33 ± 5.19	1.38 ± 0.38	0.21 ± 0.04
Mitochondria	0.40 ± 0.07	4.46 ± 0.31	1.19 ± 0.12	0.48 ± 0.15	3.64 ± 1.73	12.16 ± 12.86	4.99 ± 0.94	3.12 ± 0.27

Values are means \pm SD; four separate determinations for each substrate. TMPD, *N,N,N',N'*-tetramethyl-*p*-phenylene diamine dihydrochloride; c_{50} , cytochrome *c* concentration at which flux through the pathway of succinate respiration is stimulated by 50%; ΔJ_{max} , maximum net flux; ΔJ_{c_0} , flux at zero added cytochrome *c* concentration; $K'_{m,h}$, apparent Michaelis-Menten constant, high affinity; $\Delta V_{\text{max,h}}$, maximum net velocity, high affinity; $K'_{m,l}$, apparent K_m , low affinity; $\Delta V_{\text{max,l}}$, maximum net velocity, low affinity; V_{c_0} , velocity at zero added cytochrome *c* concentration. Respiration measured at 30°C, 1 mmol/l ADP and 0–87 $\mu\text{mol/l}$ cytochrome *c*, with 10 mmol/l succinate and 0.5 $\mu\text{mol/l}$ rotenone, or 0.5 mmol/l TMPD, 2 mmol/l ascorbate, and 5 $\mu\text{mol/l}$ antimycin A. For permeabilized fibers, J , V and v are given in $\text{nmol O}_2 \cdot \text{s}^{-1} \cdot \text{mg}^{-1}$ dry wt of fibers; for mitochondria, J , V and v are given in $\text{nmol O}_2 \cdot \text{s}^{-1} \cdot \text{mg}^{-1}$ mitochondrial protein (from Ref. 13). * $P < 0.05$, significantly different from $K'_{m,h}$ of mitochondria.

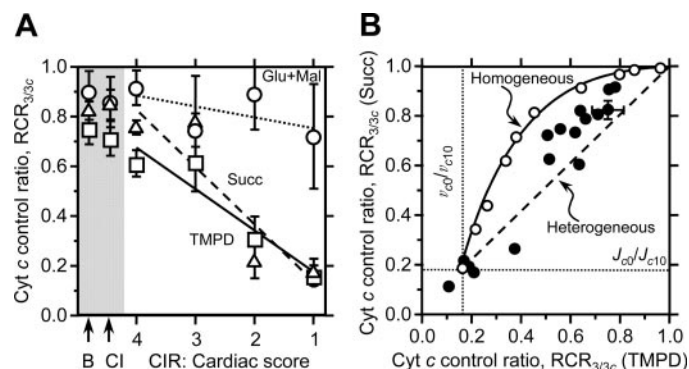


Fig. 5. Extent and heterogeneity of cytochrome *c* release after CIR. **A**: cytochrome *c* control ratio (ratio of state 3 and 3*c* respiration, RCR_{3/3c}) after CIR as a function of cardiac score. RCR_{3/3c} was measured with glutamate+malate (circles), succinate (triangles) and TMPD+ascorbate (squares). **B**: cytochrome *c* control ratio, RCR_{3/3c} with succinate (Succ) versus TMPD+ascorbate. The effect of cytochrome *c* release after CI and CIR (solid symbols) is compared with the effect of simulated cytochrome *c* depletion/titration. Open symbols show average respirometric data points from cytochrome *c* kinetics. The full line was calculated on the basis of kinetic parameters (Table 1) and represents a model of cytochrome *c* release homogeneously affecting all mitochondria. For the theoretical case of heterogeneous cytochrome *c* release, the relationship between RCR_{3/3c}(Succ) and RCR_{3/3c}(TMPD) is linear (dashed line). Closed circles represent results for individual hearts. Baseline control hearts are averaged (closed circles with SD bars; *n* = 7).

canine heart (43), and to 85% after ≥ 48 h of cold preservation of the pig liver (30).

NADH-linked respiration and cytochrome *c* stimulation remained at baseline levels after CI, whereas with severe complex I damage, the stimulatory effect of cytochrome *c* and uncoupling correlated closely with loss of contractile function after CIR. This suggests that complex I and the mitochondrial membranes are specific targets of reperfusion injury. Importantly, during normothermic reperfusion of the heart, ROS production and intracellular calcium levels increase, ATP levels are low, and inorganic phosphate concentrations are high, the combination of which is effective for permeability transition of the inner mitochondrial membrane (2, 18, 23). As a result, oxidative phosphorylation becomes uncoupled and the mitochondrial membrane potential collapses.

Cytochrome *c* release as a result of a damage of the outer mitochondrial membrane represents an early event in ischemia-reperfusion injury of the heart (3, 4, 22). The addition of cytochrome *c* to ischemic mitochondria not only restores the respiratory chain activity inhibited by the lack of cytochrome *c* (4, 22) but increases the rates of phosphorylation and proton leak (4). Because a direct stimulatory effect of cytochrome *c* on these two systems is improbable, the observed stimulation was explained by possible heterogeneity of mitochondrial damage, with general activation of electron transport of a mitochondrial subpopulation lacking cytochrome *c* (4). In the case of heterogeneity, where a different mitochondrial subpopulation with respect to cytochrome *c* content may exist (see below), respiration is even more sensitive to the overall mitochondrial release of cytochrome *c*. Because of the respiratory stimulation by cytochrome *c*, uncoupling and decline of NADH-linked respiration were observed only after reperfusion, and these injuries are possibly connected. Elevated ROS production during reperfusion may be considered as a common cause for

these multiple damages. Importantly, defective complex I after CIR can per se act as a generator of ROS in the heart (20), which then contributes to the induction of cytochrome *c* release. Cytochrome *c* release, in turn, stimulates mitochondrial superoxide formation and may thus amplify the effect of complex I damage (5). Furthermore, depletion of the main intracellular antioxidant glutathione contributes to both mitochondrial cytochrome *c* release (11) and complex I damage by direct oxidation of essential thiol groups (21) or by reaction with the product of lipid peroxidation (36). Oxidative stress during reperfusion leads to peroxidation of the phospholipid cardiolipin in the inner mitochondrial membrane (45). Peroxidation of cardiolipin may induce cytochrome *c* detachment from the inner mitochondrial membrane and release into the extramitochondrial environment (39, 45). The localized destruction of cardiolipin at sites of free radical production may explain the distinct sensitivities of different respiratory complexes to the same source of damage.

Mitochondria play a key role in the induction of apoptosis by release of cytochrome *c* (24, 26). Comparable to our findings, cytochrome *c* release leads to a rapid decrease of respiration rates in Jurkat cells undergoing Fas-mediated apoptosis (25). The sensitivity of oxidative phosphorylation to cytochrome *c* release depends, however, on simultaneous critical enzymatic defects and uncoupling, as observed after CIR. Corresponding to the differential effects of CI and CIR on respiratory cytochrome *c* control observed in our model, ischemia-reperfusion but not ischemia alone induces myocardial apoptosis (15). Importantly, warm ischemia alone leads to cytochrome *c* release and activation of the apoptotic program (3, 34). In line with analyses of gene expression (37), however, our present findings point to a specific protective effect of hypothermia on cytochrome *c* preservation during ischemia. In addition, hypothermic organ reperfusion reduces myocardial injury (17). Apoptosis is an active and energy consuming process involving regulatory genes, signal transduction, and biochemical effectors. Progression of apoptosis is, therefore, significantly dependent on ATP levels. If ATP levels fall profoundly, necrotic cell death occurs, whereas maintenance of critical ATP level allows apoptosis to proceed as the mechanism of cell death. Restoration of the ATP pool after its depletion prevents necrosis and reestablishes the execution of apoptosis (31). If cytochrome *c* depletion inhibits oxidative phosphorylation, cytochrome *c* levels are decisive in the switching between apoptosis and necrosis.

Importantly, c_{50} with succinate was identical in two different models of cytochrome *c* depletion, hypoosmotically treated myocardial fibers (present study) and digitonin-treated heart mitochondria (Table 1; Ref. 13). Cytochrome *c* kinetics was monophasic with succinate but biphasic with TMPD+ascorbate under identical incubation conditions. This difference can be explained by the high excess capacity and low flux control of cytochrome *c* oxidase in respiration with succinate versus TMPD+ascorbate (13), but other mechanisms require consideration and may be complementary, such as differences in the redox state of cytochrome *c*. Oxidized cytochrome *c* has a higher affinity to the inner mitochondrial membrane than its reduced form (7), there are two distinct pools of loosely and tightly bound mitochondrial cytochrome *c* (39), and the mitochondrial redox state regulates cytochrome *c* release.

We applied our results on cytochrome *c* kinetics of respiration to simulate various degrees of cytochrome *c* depletion. Cytochrome *c* added to fibers depleted of cytochrome *c* yields graded and homogeneous cytochrome *c* depletion throughout the mitochondrial population. Stimulation by the addition of cytochrome *c* to these homogeneously depleted fibers yielded a characteristic nonlinear relationship between $RCR_{3/3c}$ for succinate and TMPD, which was significantly different from the more linear pattern and thus highly heterogeneous distribution observed with CIR injured myocardial fibers (Fig. 5B). This result is consistent with reports on heterogeneous cytochrome *c* release after warm ischemia (4) and apoptosis (8). Selective decline of oxidative phosphorylation and cytochrome *c* depletion after global warm ischemia (45 min) have been demonstrated in subsarcolemmal but not in interfibrillar mitochondria in perfused rabbit heart model (34). An alternative interpretation of our data on the relative cytochrome *c* stimulation for succinate versus TMPD respiration (Fig. 5B) is afforded by a potential effect on cytochrome *c* kinetics after CIR. Importantly, however, cytochrome *c* kinetics remains unchanged after warm ischemia (34). Cellular mosaicism of respiratory changes and heterogeneous cytochrome *c* release have been demonstrated by the separation of Jurkat cells undergoing anti-Fas-triggered apoptosis (16). Similarly, fluorescence confocal imaging and flow cytometry reveal subcellular heterogeneity of mitochondria (29). Mitochondria of several cell types are heterogeneous with respect to membrane potential, calcium loading and susceptibility to permeability transition (6).

Under conditions of heterogeneous cytochrome *c* depletion and reduced complex I activity, the lack of respiratory control of cytochrome *c* in NADH-linked respiration (Fig. 2D) provides indirect evidence for the close link between these injuries. The occurrence of metabolically significant cytochrome *c* release in a subpopulation of mitochondria that is not affected by complex I injury would be detected by cytochrome *c* stimulation of respiration. The decline of complex I activity with loss of cardiac function, therefore, can be most simply explained by an increasing fraction of mitochondria devoid of complex I activity and of cytochrome *c*, with a mitochondrial fraction remaining intact and capable of aerobic ATP production. Indeed, mitochondrial heterogeneity during apoptosis has been demonstrated with respect to the preservation of mitochondrial membrane potential, which is required for ATP production (27). We conclude that various mitochondrial defects induced by CIR correlated with cytochrome *c* release and were thus heterogeneously distributed between subpopulations of mitochondria.

Cytochrome *c* release mediated by permeability transition is suppressed by cyclosporin A (2, 18) and minocycline (51). These drugs may thus be considered as mediators of cardioprotection in organ preservation. Our evidence for multiple mitochondrial injury and limitation of respiratory flux by the pronounced complex I defect after cold storage and reperfusion, however, suggests that only a combination of several protective strategies will result in successful prolongation of cardiac storage. This conclusion is supported by the fact that several molecular and physiologically adaptive responses are triggered by preconditioning (9, 10, 49). A combinatorial approach, therefore, extends the established concept on multiple effectors contained in the presently available organ pres-

ervation solutions. Thus a better understanding of the pathophysiological mechanisms responsible for mitochondrial damage in the ischemic-reperfused myocardium provides the basis for novel multifactorial intervention strategies aimed at improving heart preservation and enhancing cardiac recovery after prolonged cold ischemia.

ACKNOWLEDGMENTS

We are grateful for the technical assistance of M. Schneider.

REFERENCES

1. Appaix F, Minatchy M, Riva-Lavielle C, Olivares J, Antonsson B, and Saks VA. Rapid spectrophotometric method for quantitation of cytochrome *c* release from isolated mitochondria or permeabilized cells revisited. *Biochim Biophys Acta* 1457: 175–181, 2000.
2. Bernardi P, Petronilli V, Di Lisa F, and Forte M. A mitochondrial perspective on cell death. *Trends Biochem Sci* 26: 112–117, 2001.
3. Borutaite V, Budriunaite A, Morkuniene R, and Brown GC. Release of mitochondrial cytochrome *c* and activation of cytosolic caspases induced by myocardial ischaemia. *Biochim Biophys Acta* 1537: 101–109, 2001.
4. Borutaite V, Morkuniene R, Budriunaite A, Krasauskaite D, Ryselis S, Toleikis A, and Brown GC. Kinetic analysis of changes in activity of heart mitochondrial oxidative phosphorylation system induced by ischemia. *J Mol Cell Cardiol* 28: 2195–2201, 1996.
5. Cai J and Jones DP. Superoxide in apoptosis. Mitochondrial generation triggered by cytochrome *c* loss. *J Biol Chem* 273: 11401–11404, 1998.
6. Collins TJ, Berridge MJ, Lipp P, and Bootman MD. Mitochondria are morphologically and functionally heterogeneous within cells. *EMBO J* 21: 1616–1627, 2002.
7. Cortese JD, Voglino AL, and Hackenbrock CR. Persistence of cytochrome *c* binding to membranes at physiological mitochondrial intermembrane space ionic strength. *Biochim Biophys Acta* 1228: 216–228, 1995.
8. D'Herde K, De Prest B, Mussche S, Schotte P, Beyaert R, Coster RV, and Roels F. Ultrastructural localization of cytochrome *c* in apoptosis demonstrates mitochondrial heterogeneity. *Cell Death Differ* 7: 331–337, 2000.
9. Dos Santos P, Kowaltowski AJ, Laclau MN, Seetharaman S, Paucet P, Boudina S, Thambo JB, Tariosse L, and Garlid KD. Mechanisms by which opening the mitochondrial ATP-sensitive K^+ channel protects the ischemic heart. *Am J Physiol Heart Circ Physiol* 283: H284–H295, 2002.
10. Dzeja PP, Bast P, Ozcan C, Valverde A, Holmuhamedov EL, Van Wylen DGL, and Terzic A. Targeting nucleotide-requiring enzymes: implications for diazoxide-induced cardioprotection. *Am J Physiol Heart Circ Physiol* 284: H1048–H1056, 2003.
11. Ghibelli L, Coppola S, Fanelli C, Rotilio G, Civitareale P, Scovassi AI, and Ciriolo MR. Glutathione depletion causes cytochrome *c* release even in the absence of cell commitment to apoptosis. *FASEB J* 13: 2031–2036, 1999.
12. Gnaiger E. Bioenergetics at low oxygen: dependence of respiration and phosphorylation on oxygen and adenosine diphosphate supply. *Respir Physiol* 128: 277–297, 2001.
13. Gnaiger E and Kuznetsov AV. Mitochondrial respiration at low levels of oxygen and cytochrome *c*. *Biochem Soc Trans* 30: 242–248, 2002.
14. Gnaiger E, Kuznetsov AV, Schneeberger S, Seiler R, Brandacher G, Steurer W, and Margreiter R. Mitochondria in the cold. In: *Life in the Cold*, edited by Heldmaier G and Klingenspor M. Berlin: Springer, 2000, p. 431–442.
15. Gottlieb RA, Bursleson KO, Kloner RA, Babior BM, and Engler RL. Reperfusion injury induces apoptosis in rabbit cardiomyocytes. *J Clin Invest* 94: 1621–1628, 1994.
16. Hajek P, Villani G, and Attardi G. Rate-limiting step preceding cytochrome *c* release in cells primed for Fas-mediated apoptosis revealed by analysis of cellular mosaicism of respiratory changes. *J Biol Chem* 276: 606–615, 2001.
17. Hale SL, Dae MW, and Kloner RA. Hypothermia during reperfusion limits no-reflow injury in a rabbit model of acute myocardial infarction. *Cardiovasc Res* 59: 715–722, 2003.
18. Halestrap AP, Kerr PM, Javadov S, and Woodfield KY. Elucidating the molecular mechanism of the permeability transition pore and its role in reperfusion injury of the heart. *Biochim Biophys Acta* 1366: 79–94, 1998.

19. **Hatefi Y and Stiggall DL.** Preparation and properties of NADH: cytochrome c oxidoreductase (complex I–III). *Methods Enzymol* 53: 5–10, 1978.
20. **Ide T, Tsutsui H, Kinugawa S, Utsumi H, Kang D, Hattori N, Uchida K, Arimura K, Egashira K, and Takeshita A.** Mitochondrial electron transport complex I is a potential source of oxygen free radicals in the failing myocardium. *Circ Res* 85: 357–363, 1999.
21. **Jha N, Jurma O, Lalli G, Liu Y, Pettus EH, Greenamyre JT, Liu RM, Forman HJ, and Andersen JK.** Glutathione depletion in PC12 results in selective inhibition of mitochondrial complex I activity. *J Biol Chem* 275: 26096–26101, 2000.
22. **Kay L, Daneshrad Z, Saks VA, and Rossi A.** Alteration in the control of mitochondrial respiration by outer mitochondrial membrane and creatine during heart preservation. *Cardiovasc Res* 34: 547–556, 1997.
23. **Kerr PM, Suleiman MS, and Halestrap AP.** Reversal of permeability transition during recovery of hearts from ischemia and its enhancement by pyruvate. *Am J Physiol Heart Circ Physiol* 276: H496–H502, 1999.
24. **Kluck RM, Bossy-Wetzell E, Green DR, and Newmeyer DD.** The release of cytochrome c from mitochondria: a primary site for Bcl-2 regulation of apoptosis. *Science* 275: 1132–1136, 1997.
25. **Krippner A, Matsuno-Yagi A, Gottlieb RA, and Babior BM.** Loss of function of cytochrome c in Jurkat cells undergoing fas-mediated apoptosis. *J Biol Chem* 271: 21629–21636, 1996.
26. **Kroemer G and Reed JC.** Mitochondrial control of cell death. *Nat Med* 6: 513–519, 2000.
27. **Krysko DV, Roels F, Leybaert L, and D’Herde K.** Mitochondrial transmembrane potential changes support the concept of mitochondrial heterogeneity during apoptosis. *J Histochem Cytochem* 49: 1277–1284, 2001.
28. **Kuwabara M, Takenaka H, Maruyama H, Onitsuka T, and Hamada M.** Effect of prolonged hypothermic ischemia and reperfusion on oxygen consumption and total mechanical energy in rat myocardium: participation of mitochondrial oxidative phosphorylation. *Transplantation* 64: 577–583, 1997.
29. **Kuznetsov AV, Mayboroda O, Kunz D, Winkler K, Schubert W, and Kunz WS.** Functional imaging of mitochondria in saponin-permeabilized mice muscle fibers. *J Cell Biol* 140: 1091–1099, 1998.
30. **Kuznetsov AV, Strobl D, Ruttman E, Konigsrainer A, Margreiter R, and Gnaiger E.** Evaluation of mitochondrial respiratory function in small biopsies of liver. *Anal Biochem* 305: 186–194, 2002.
31. **Leist M, Single B, Castoldi AF, Kuhle S, and Nicotera P.** Intracellular adenosine triphosphate (ATP) concentration: a switch in the decision between apoptosis and necrosis. *J Exp Med* 185: 1481–1486, 1997.
32. **Lesnefsky EJ, Guduz TI, Migita CT, Ikeda-Saito M, Hassan MO, Turkaly PJ, and Hoppel CL.** Ischemic injury to mitochondrial electron transport in the aging heart: damage to the iron-sulfur protein subunit of electron transport complex III. *Arch Biochem Biophys* 385: 117–128, 2001.
33. **Lesnefsky EJ, Moghaddas S, Tandler B, Kerner J, and Hoppel CL.** Mitochondrial dysfunction in cardiac disease: ischemia-reperfusion, aging, and heart failure. *J Mol Cell Cardiol* 33: 1065–1089, 2001.
34. **Lesnefsky EJ, Tandler B, Ye J, Slabe TJ, Turkaly J, and Hoppel CL.** Myocardial ischemia decreases oxidative phosphorylation through cytochrome oxidase in subsarcolemmal mitochondria. *Am J Physiol Heart Circ Physiol* 273: H1544–H1554, 1997.
35. **Li C and Jackson RM.** Reactive species mechanisms of cellular hypoxia-reoxygenation injury. *Am J Physiol Cell Physiol* 282: C227–C241, 2002.
36. **Lucas DT and Szveda LL.** Cardiac reperfusion injury: aging, lipid peroxidation, and mitochondrial dysfunction. *Proc Natl Acad Sci USA* 95: 510–514, 1998.
37. **Ning XH, Chen SH, Xu CS, Li L, Yao LY, Qian K, Krueger JJ, Hytti OM, and Portman MA.** Hypothermic protection of the ischemic heart via alterations in apoptotic pathways as assessed by gene array analysis. *J Appl Physiol* 92: 2200–2207, 2002.
38. **Ono K and Lindsey ES.** Improved technique of heart transplantation in rats. *J Thorac Cardiovasc Surg* 57: 225–229, 1969.
39. **Ott M, Robertson JD, Gogvadze V, Zhivotovsky B, and Orrenius S.** Cytochrome c release from mitochondria proceeds by a two-step process. *Proc Natl Acad Sci USA* 99: 1259–1263, 2002.
40. **Renner K, Kofler R, and Gnaiger E.** Mitochondrial function in glucocorticoid triggered T-ALL cells with transgenic bcl-2 expression. *Mol Biol Rep* 29: 97–101, 2002.
41. **Saks VA, Kuznetsov AV, Khuchua ZA, Vasilyeva EV, Belikova JO, Kesvatera T, and Tiivel T.** Control of cellular respiration in vivo by mitochondrial outer membrane and by creatine kinase. A new speculative hypothesis: possible involvement of mitochondrial-cytoskeleton interactions. *J Mol Cell Cardiol* 27: 625–645, 1995.
42. **Salvioli S, Dobrucki J, Moretti L, Troiano L, Fernandez MG, Pinti M, Pedrazzi J, Franceschi C, and Cossarizza A.** Mitochondrial heterogeneity during staurosporine-induced apoptosis in HL60 cells: analysis at the single cell and single organelle level. *Cytometry* 40: 189–197, 2000.
43. **See YP, Weisel RD, Mickle DA, Teoh KH, Wilson GJ, Tumiati LC, Mohabeer MK, Madonik MM, Axford-Gatley RA, and Salter DR.** Prolonged hypothermic cardiac storage for transplantation. The effects on myocardial metabolism and mitochondrial function. *J Thorac Cardiovasc Surg* 104: 817–824, 1992.
44. **Semenza GL.** Cellular and molecular dissection of reperfusion injury: ROS within and without. *Circ Res* 86: 117–118, 2000.
45. **Shidoji Y, Hayashi K, Komura S, Ohishi N, and Yagi K.** Loss of molecular interaction between cytochrome c and cardiolipin due to lipid peroxidation. *Biochem Biophys Res Commun* 264: 343–347, 1999.
46. **Srere PA.** Citrate synthase. *Methods Enzymol* 13: 3–11, 1969.
47. **Stringham JC, Southard JH, Hegge J, Triemstra L, Fields BL, and Belzer FO.** Limitations of heart preservation by cold storage. *Transplantation* 53: 287–294, 1992.
48. **Vanden Hoek TL, Qin Y, Wojcik K, Li CQ, Shao ZH, Anderson T, Becker LB, and Hamann KJ.** Reperfusion, not simulated ischemia, initiates intrinsic apoptosis injury in chick cardiomyocytes. *Am J Physiol Heart Circ Physiol* 284: H141–H150, 2003.
49. **Williams RS and Benjamin IJ.** Protective responses in the ischemic myocardium. *J Clin Invest* 106: 813–818, 2000.
50. **Yano H, Takenaka H, Onitsuka T, Koga Y, and Hamada M.** Cardioplegic effect of University of Wisconsin solution on hypothermic ischemia of rat myocardium assessed by mitochondrial oxidative phosphorylation. *J Thorac Cardiovasc Surg* 106: 502–510, 1993.
51. **Zhu S, Stavrovskaya IG, Drozda M, Kim BY, Ona V, Li M, Sarang S, Liu AS, Hartley DM, Wu DC, Gullans S, Ferrante RJ, Przedborski S, Kristal BS, and Friedlander RM.** Minocycline inhibits cytochrome c release and delays progression of amyotrophic lateral sclerosis in mice. *Nature* 417: 74–78, 2002.